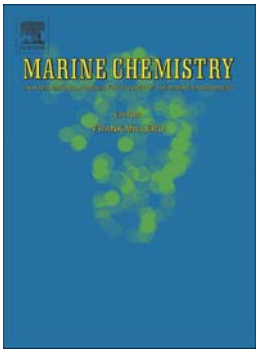

Mobility of mercury in contaminated marine sediments: biogeochemical pathways

Elvira Oliveri, Daniela Salvagio Manta, Maria Bonsignore, Simone Cappello, Giorgio Tranchida, Emanuela Bagnato, Nadia Sabatino, Santina Santisi, Mario Sprovieri

PII: S0304-4203(16)30092-5
DOI: doi: 10.1016/j.marchem.2016.07.002
Reference: MARCHE 3385

To appear in: *Marine Chemistry*

Received date: 11 March 2016
Revised date: 24 June 2016
Accepted date: 5 July 2016

Please cite this article as: Oliveri, Elvira, Manta, Daniela Salvagio, Bonsignore, Maria, Cappello, Simone, Tranchida, Giorgio, Bagnato, Emanuela, Sabatino, Nadia, Santisi, Santina, Sprovieri, Mario, Mobility of mercury in contaminated marine sediments: biogeochemical pathways, *Marine Chemistry* (2016), doi: 10.1016/j.marchem.2016.07.002

Mobility of mercury in contaminated marine sediments: biogeochemical pathways

Elvira Oliveri[a]*, Daniela Salvagio Manta[a], Maria Bonsignore[a], Simone Cappello[b], Giorgio Tranchida [a], Emanuela Bagnato[a], Nadia Sabatino[a], Santina Santisi[b], Mario Sprovieri[a]

[a]Institute for Coastal Marine Environment (IAMC), CNR, Via Del Mare 3, 91021 Torretta Granitola, Campobello di Mazara (TP) Italy

[b]Institute for Coastal Marine Environment (IAMC), CNR, Spianata S.Raineri 86, 98122 Messina, Italy

[c]Institute for Coastal Marine Environment (IAMC), CNR, Calata Porta di Massa, 80133 Napoli, Italy

Elvira Oliveri * *(Corresponding author)*: Institute for Coastal and Marine Environment (IAMC) – CNR, Via del Mare, 3, 91021 Torretta Granitola, Campobello di Mazara (TP), Italy
email address: elvira.oliveri@iamc.cnr.it
Telephone: *+39 0924 40600;* fax**:** *+39 0924 40445*

Abstract

The availability of dissolved inorganic mercury (DHg) in sediment pore water is a crucial step for the mechanisms of methylmercury (MeHg) generation in the aquatic system. The geochemical form of Hg in sediments and the redox-controlled microbial reactions taking place during *early diagenesis* regulate the pool of DHg and, consequently, the bioavailability of Hg for methylation. Here, we report new evidence on the biogeochemical mechanisms controlling the pool of DHg in sediment pore water from two box-cores collected from Augusta Bay (Sicily), a marine coastal zone heavily contaminated by chlor-alkali discharges. The content of the total Hg (THg) in the studied sediments (4.13÷22.2 mg Kg^{-1}) is largely present as an "immobile" phase, while the labile fractions account for minor percentages (<2%). Despite the predominance of Hg "immobile" forms, depth profiles of the pore water suggest relevant DHg production (up to 226 ng L^{-1}) mainly in the deeper levels of the investigated sedimentary column. Specifically, most of the THg appears to be partially mobilized in the "Fe-Mn reduction" zone, as clearly suggested by significant correlations between DHg and dissolved Fe-Mn concentrations in the pore water. The irregular vertical distribution of SO_4^{2-}, with evident enrichment in the Fe-Mn reduction zone, could also indicate mechanisms of sulphate generation by sulphide oxidation. Specific microbial populations identified in the sediments appear dominated by chemolithoautotrophic sulphur oxidizing bacteria (SOB, genera *Sulfurovum* and *Thioalkalispira*) which could drive the microbial oxidation of sulphides and support, with effects of Mn-Fe oxide reduction, processes of Hg mobilization.

Keywords: mercury, Hg bioavailability, marine sediment, pore water, anaerobic sulphide oxidation, Augusta Bay.

1. Introduction

Coastal marine sediment is often a major repository of anthropogenic mercury (Hg), but biogeochemical reactions taking place during processes of *early diagenesis* can mobilize and definitively geochemically transform this pollutant (Bothener et al., 1980; Gagnon et al., 1997; 1996; Gobeil and Cossa, 1993; Jonsson et al., 2014) into more available and dangerous forms (e.g., the highly toxic methylmercury, MeHg; Barkay and Wagner-Döbler, 2005). The dynamics of Hg accumulation in marine sediment are primarily controlled by organic matter which is the most efficient Hg scavenger in the water column (Guentzel et al., 1996; Ravichandran, 2004), although iron and manganese oxides can also have an important role (Gobeil and Cossa, 1993; Feyte 2010). When sediment undergoes redox changes because of organic matter mineralization (e.g., Froelich et al.,1979), the Hg bound to organic matter or Mn-Fe oxides can be released in pore water (Cossa and Gobeil, 2000; Gagnon et al., 1997; Gobeil and Cossa, 1993). In anoxic sulphuric sediments, the reaction between Hg and sulphide (H_2S) can lead to the precipitation of highly stable Hg-sulphides such as cinnabar (HgS, Huerta-Diaz and Morse, 1992; Revis et al. 1989). In this case, the factors controlling the solubility of Hg-sulphides will also influence the partitioning of Hg between sediment and pore water (Benoit et al. 1999a, b; Fitzgerald et al., 2007; Skyllberg, 2012). However, the excessive activity of sulphide (HS^-) and/or the generation of zero-valent sulphur (S^0) can promote HgS solubility and, consequently, induce effects of the mobility and availability of Hg in anoxic sediment (Jay et al., 2000; Paquette and Heltz, 1997). This mechanism is responsible for the high concentrations of soluble mercury species that are often found in anoxic zones of the bottom sediment (Nakanishi et al., 1989; Fergusson, 1990). In order to adapt to the presence of mercury, microorganisms can affect the mobility of Hg in a variety of metabolic pathways (Barkay and Wagner-Döbler 2005). It is widely recognized that sulphate reducing bacteria (SRB) can generate methylmercury (MeHg) in natural habitats like salt marshes and estuarine and freshwater sediment (Benoit et al., 2001a; Compeau & Bartha, 1985; Gilmour et al., 1992; King et al., 2000; Ranchou-Peyruse et al., 2009, Schartup, 2013). In sulphuric environments characterized by the precipitation of abundant Hg-sulphide (e.g. cinnabar), the polysulphide-induced solubilization of cinnabar can regulate availability for Hg methylation by SRB (Benoit et al., 2001b). In extreme environments such as deep sea vents and hot sulphuric springs, some microorganisms, e.g. sulphur oxidizing bacteria (SOB), outlive Hg through the sulphide oxidation of cinnabar deposits (Chatziefthimiou et al., 2007; Simbahan et al., 2005; Vetriani et al., 2005). Overall, the interactions between microbes and Hg-species facilitate the recycling of Hg and its bioavailability in the environment (Barkay and Wagner-Döbler 2005).

This paper examines the main factors controlling the early diagenetic re-mobilization of Hg in sediments collected from the coastal marine area of Augusta Bay (eastern Sicily, Italy). In particular, the depth distributions of total Hg (THg) and the main parameters (grain size, mineralogy, and organic carbon) were analyzed in two sediment cores, to delineate the physico-chemical characteristics of the sediment matrix influencing Hg distribution in the Augusta Bay sediments. The sequential selective extraction (SSE) procedure was used to examine the main Hg solid-phases in the investigated sediment, with a view to evaluating the presence of mobile and potentially bioavailable species. Pore water chemistry was determined and analyzed for total Hg, Fe, Mn and SO_4^{2-} concentrations in order to study the predominant relationships between the release of Hg and the vertical change of the redox zone within the sediment. Pioneering microbiology exploration allowed us to identify the Hg-resistant microbial communities that inhabit the investigated environment and their pressure on Hg-remobilization in the Augusta Bay sediments.

2. Materials and Methods

2.1. Study area

Augusta Bay occupies a coastal area of about 30 km^2 in eastern Sicily (southern Italy), and is one of the most industrialized and polluted areas in the Mediterranean Sea (Fig. 1a). The harbour area, delimited in the northern sector by the town of Augusta and closed to the south and east by artificial dams, is 8 km long and 4 km wide, with a mean water depth about of 15 m (ICRAM, 2008). Since the early 1960s, an important industrialization process has adversely affected the area (with many chemical and petrochemical plants, oil refineries, etc.), but the most dangerous activity was caused by chlor-alkali plant with mercury cell operating from 1958 to 2003 (ICRAM, 2008). The uncontrolled discharge of huge amounts of Hg waste in the harbour led to significant contamination of the bottom sediment, particularly in the SW zone where the chlor-alkali plant was located (Fig. 1b) (Bellucci, 2011; Croudace et al., 2015; ICRAM, 2008; Sprovieri et al., 2011), with evident and recently documented risks for the ecosystem and human health (Bonsignore et al., 2015, 2013; Sprovieri et al., 2011;).

2.2. Sampling

Sediments were collected using a box-corer during a cruise expedition on the R/V "*L. Dalla Porta*" in May 2011 (Fig. 1b). One box-core was acquired from each site and immediately subsampled on board using 30-cm long polyethylene tubes. Specifically, four sub cores were recovered from each site and stored at −20 °C until the geochemical analyses were conducted. Two sedimentary records were stored at +4°C for microbiological analysis. In the laboratory, two sub

cores were extruded and sliced inside a N_2 filled glove bag at 1 cm intervals down to 10 cm and at 2 cm intervals below 10 cm. A total of 17 samples from Core 8 (21 cm long) and 16 from Core 16 (22 cm long) were collected. The sediment samples were dried (T = 35 °C) and homogenised before the mineralogy phases, Total Organic Carbon (TOC) and THg were determined. An SSE procedure was carried out on sediment from two sub cores. In Particular, 3 cm slices for a total of nine samples were analyzed.

2.3 Geochemical analyses

2.3.1. Sediment

The mineralogy of the bulk samples was investigated by X-ray diffraction (XRD), using a D8 Discover Bruker equipped with a Sol-X detector. The instrumental conditions were Cu–Kα radiation and a scanning speed of 2 2°ϑ /min. The semi-quantitative analysis of the minerals was performed according to methods and data reported in Schultz (1964) and Barahona et al. (1982).

The TOC content in the sediment was determined by a Thermo Electron Flash EA 1112, after elimination of all the carbonate fractions present in the samples. Specifically, about 5 mg of bulk sediment samples were decarbonated using HCl 1M in silver cups for 24 h at $T_{ambient}$ and then dried in a oven at T=60°C. An internal standard (urea with C = 20%, N = 46%) was run every six samples.

The THg concentrations in the sediments were determined with an atomic absorption spectrophotometer using a direct mercury analyzer (Milestone_DMA-80; US-EPA 7473). A Reference Standard Material (PACS-2 Marine sediment, NRCC) was analyzed to assess accuracy (estimated to be ~7%) and precision (routinely better than 6%; RSD%, n= 3). Finally, duplicate samples (about 20% of the total number of samples) were measured to estimate reproducibility, which was better than 7%. In order to minimize the contamination risks, acid-cleaned laboratory materials were used during the sample preparation and analyses.

Details of the distribution of the Hg in the different phases of the sediment were obtained using the SSE procedure according to Bloom et al. (2003),. This method differentiates Hg species based on their geochemical behaviour, and includes i) water soluble species (F1), ii) “human stomach acid” soluble species (F2), iii) organo-chelated species (F3), iv) strong-complex species with elemental Hg and/or Hg bound to amorphous organo-sulphur or crystalline Fe/Mn oxide phases (F4), and v) low solubility compounds with Hg sulphide (F5). In order to minimise the contamination risks, all the extracting solutions (Tab. 1) were prepared by diluting *ultrapure* reagents with deionised water, and all the analytical procedures were conducted using acid-cleaned laboratory materials. The extractions were carried out in borosilicate centrifuge tubes, using ~2 g of fresh sediment and 20 ml of extracting solution (Tab. 1). Each step was performed at $T_{ambient}$, with

constant agitation, for 18 ± 3 hours. The vials were then centrifuged at 3000 rpm and the supernatant recovered. The residual sediment was re-suspended in the same extractant, re-centrifuged, and the supernatant recovered. The two obtained solutions were placed in 50 ml borosilicate vials and oxidized by adding an aliquot of BrCl solution (EPA 1631). Each step included three rinse cycles (two with 5 ml of the same extraction solution and one with MilliQ water). After the rinse, the samples were re-suspended in the next extractant, and the entire process was repeated. THg concentrations in the F1, F2 and F3 fractions were determined using a DMA-80 according to the EPA 7473 analytical procedure, while the F4 and F5 fractions were analyzed by atomic emission spectrometry (ICP-AES, Thermo-icap 6000). The effectiveness of the method was evaluated on the $\Sigma Hg_{step}/HgT_{sample}$ ratio, with Hg_{step}= the sum of the Hg concentrations determined in each step and HgT_{sample}= the THg determined in the bulk sample ($\Sigma Hg/HgT$ = 75 ÷ 117%).

2.3.2. Pore water

Extraction of the pore water was performed by centrifugation (3500 rpm for 40 min) and following filtration (0.45 μm) under an N_2 atmosphere (Mason et al., 1998). The dissolved total Hg (DHg) concentration was determined in the obtained extracts using a direct mercury analyzer, (Milestone_DMA-80; US-EPA 7473), after oxidation with a 0.05% (w/v) bromine monochloride (BrCl) fresh solution (0.5 mL/100 mL sample; US-EPA 1631). Blank, duplicate and spiked samples (about 20% of the samples) were analyzed to assess the detection limit (d.l.= 1.9 ng L^{-1}; 3σ of the reagent blank), reproducibility (better than 10%), and accuracy (%recovery= 85÷110%) of the method. Dissolved total Fe and Mn concentrations were determined by ICP AES (Thermo ICAP 6000; EPA 6010b). Blank, spiked and duplicate samples (about 20% of the samples) were analyzed to assess the detection limit (d.l.= 0.3 and 0.7 ng L^{-1} for Mn and Fe, respectively; 3σ of the reagent blank) and reproducibility (between 5÷10%) of the method. SO_4^{2-} was determined using a Thermo Scientific Dionex ICS-1100 Ion Chromatography System equipped with an autosampler according to the APAT 4020 method. An aliquot of 5 ml of untreated sample (diluited1:1000) was directly injected into the vials and closed with a cap filter (0.2 μm) included in the autosampler (Dionex AS-DV Ship Kit). Concentrations of SO_4^{2-} in seawater were determined in single IC runs. The achieved detection limit was 0.1 mg/L sulfate.

2.4 Microbiology

The microbiology exploration was performed on the basis of two main criteria: i) we considered two deep sedimentary levels characterized by different degrees of Hg contamination; ii) both sedimentary levels were at the depth where the most important release of DHg in the pore waters was identified (Tab. 2).

To monitor the quantitative abundance of the microbial population present in the studied samples, measures of direct bacterial count (DAPI), cultivable bacteria (CFU), Most Probable Number (MPN) were carried out. The structure of the microbial population was also determined using a taxonomic analysis (cloning library of 16S crDNA). Except for this analysis of the microbial population, all parameters detected were measured three times.

2.4.1. Dispersion procedures and bacterial counting (DAPI)

Prior to dispersion, the samples were incubated for at least 15 min with Tween 80 (final concentration, 1 mg L^{-1}). In accordance with Kuwae and Hosokawe (1999), an ultrasonic cleaner (Branson 1200, Milan) was used for the bacterial dispersion from the sediment (20 min). After centrifugation (8 min at 8000 xg) and collection of the water-tween 80 phase, cell counts were performed by DAPI (Sigma-Aldrich S.r.L., Milan, Italy) staining on samples fixed with formaldehyde (2% final concentration). The samples were prepared as previously reported (Cappello et al. 2007; Zampino et al. 2004). The slides were examined by epifluorescence with an Axioplan 2 Imaging (Zeiss; Carl Zeiss Inc., Thornwood, N.Y.) microscope. All the results were expressed as the number of cells per ml^{-1}.

2.4.2. Cultivable bacteria (CFU)

To enumerate the total heterotrophic bacteria and oil-degrading bacteria, dispersion (carried out as previously described) of the sediment was serially diluted in a sterile physiological solution and plated on a Marine agar 2216 medium (Difco S.p.a, Milan, Italy), ONR7a (Dyksterhouse et al., 1995) and ONR7a added to sterilized crude oil (Arabian Ligth Crude Oil) as a unique energy and/or carbon source. Culture media and crude oil were autoclaved separately for 20 min at 120°C. All the agar plates were incubated at 25±1°C for seven days.

2.4.3. Most Probable Number (MPN)

After the dispersion procedures**,** the hydrocarbon-degrading bacteria were enumerated by a miniaturized, slightly modified, MPN method (Cappello et al., 2007). The MPN of the hydrocarbon-degrading microorganisms was determined from the appropriate MPN tables according to the American Public Health Association (A.P.H.A. 1992).

2.4.4. Molecular and taxonomic analysis (cloning library of 16S crDNA).

Extraction of total RNA was performed using the MasterPure Complete DNA&RNA Purification Kit (Epicenter, Biotechnologies, Madison, WI) according to the manufacturer's protocol. The

rRNA-crDNA heteroduplex was synthesized by reverse transcription using random primer (hexamer) oligonucleotides and SuperScript II RNase H-free reverse transcriptase (Life Technologies). RT amplification was realized using the protocol recommended by the manufacturer, with 20 µl reaction mixtures containing 200 µM of deoxynucleoside triphosphate, 5 µM of hexamer, and 50 to 100 ng of denatured RNA with a GeneAmp PCR System 2700 (Applied Biosystems Foster City, CA, USA).The thermal cycle parameters were as follows: 5 min at 65°C and 2 min at 4°C, followed by the addition of a 1× first-strand buffer and 75-U of a RNase inhibitor and heating at 37°C for 2 min. Reverse transcriptase was added prior to a 50-min incubation at 42°C. This reaction was then stopped at 80°C for 5 min. Possible DNA contamination of the RNA templates was routinely monitored by the PCR amplification of aliquots of RNA that were not reverse transcribed; no contaminating DNA was detected in any of these reactions. The primers used for the PCR included the reverse primer referred to above (Uni_1492R) and the 16S rRNA forward domain-specific bacteria, Bac27_F (5'-AGAGTTTGATCCTGGCTCAG-3'; Lane 1991). The PCR (initial denaturation: 5 min hot-start at 95°C; 1 min at 94°C, 1 min at 50°C, 2 min at 72°C, 30 cycles; extension: 10 min at 72°C) was performed with GeneAmp 5700 (PE Applied Biosystems, Foster City, CA, USA), using a 50 µl (total volume) mixture containing 1x solution Q (Qiagen, Hilden, Germany), a 1× Qiagen reaction buffer, 1 µM of each forward and reverse primer, 10µM dNTPs (Gibco, Invitrogen Co., Carlsbad, CA), 2.0 ml (50-100 ng) of template and 2.0 U of Qiagen Taq Polymerase (Qiagen). After gel electrophoresis of the PCR products, purified amplicons representing 16S crDNA sequences were cloned in the pGEM T-easy Vector II (Promega, Madison, Wis., USA), and inserts from the transformed E. coli DH10β colonies. After blue/white screening, randomly-picked colonies were resuspended in PCR lysis solution A without proteinase K (67 mM Tris–Cl;pH 8.8), 16 mM NH_4SO_4, 5 µM β- mercaptoethanol, 6.7 mM $MgCl_2$, and 6.7 µM EDTA (pH 8.0), and heated at 95°C for 5 min. The lysate (approximately 0.2 ng DNA) was used as the template for the PCR amplification with the primers M13F (5′-GACGTTGTAAAACGACGGC CAG-3) and M13R (5′-GAGGAAACAGCTATGAC CATG-3). The PCR products were sequenced using the Macrogen Service (Macrocen, Korea). The analysis of the sequences (1400 bp of average length) was performed as previously described by Yakimov et al. (2005). The sequence similarity of individual inserts was analyzed by the FASTA program Nucleotide Database Query available through the EMBL-European Bioinformatics Institute. The phylogenetic affiliation of the sequenced clones was performed as described by Yakimov et al. (2006).

3. Results

3.1. Sediment

3.1.1. Geochemical characterization

The studied sediments consisted of silt and clay mud with minor percentages of a sand fraction (Tab. 1). The mineralogical composition mainly consisted of calcite, clay minerals and quartz, with percentages of 25÷55%, 10÷50% and 9÷34%, respectively (Tab. 2). Hematite, plagioclase, dolomite, rhodochrosite, siderite and pyrite were the secondary minerals (percentages did not exceed 5%; Tab. 1).

The TOC values varied between 1.87% and 2.45% and between 1.89% and 2.47% in cores 8 and 16, respectively. In both cores, the values slightly decreased in the uppermost 4 cm and were rather homogeneous around an average value of 2.32% along the lower part of the cores(Fig. 2).

The THg concentrations varied between 4.31 and 7.61 mg kg^{-1} and between 12.3 and 22.1 mg kg^{-1} in cores 8 and 16, respectively (Fig. 2). The THg in Core 8 had rather steady values in the upper 13 cm and a declining trend from 14.5 cm onwards (Fig. 2), while Core 16 exhibited an increasing trend with depth (Fig. 2).

The SSE showed that most of the Hg in the solid-phase was distributed between the fractions F4 (THg-F4=80÷95%) and F5 (THg-F5= 4÷19%), while the content of THg in fractions F1 (THg-F1), F2 (THg-F2) and F3 (THg-F3) was negligible (<2%, Fig. 3a). THg-F1 and THg-F2 were easily exchangeable fractions ($HgCl_2$, $HgSO_4$, HgO), and their sum (THg-F1+THg-F2) provided an estimate of the bio-accessible Hg in the aqueous media (Bloom et al. , 2003). In the Augusta sediments, the sum (THg-F1+THg-F2) was between 0.02% and 0.14% lower than that generally reported for other similar marine sediments (1.5 %, Bloom et al., 2003; 0.4%, Covelli et al., 2011). The F3 fraction basically consisted of Hg associated with organic matter and, possibly, minor amounts of Hg-methylated species (Bloom et al., 2003). In all the samples, THg-F3 represented a minor fraction (<1.10%; Fig. 3a) that was again lower than that found in other contaminated sediments (Covelli et al., 2009; 2011). THg-F4 was the predominant Hg-solid phase in the Augusta sediments (Fig. 3a). This fraction prevalently contained free elemental mercury (Hg^0), although Hg(I), Hg bound to crystalline phases, such as Fe-Mn oxides or Hg bound to amorphous organo-sulfur phases, could occur (Bloom et al., 2003). According to Bloom et al. (2003), high contents of THg-F4 may indicate significant levels of native Hg^0 if the THg measured in steps F1-F3 accounts for about 50 μg L^{-1} (Hg^0 water solubility; Bloom et al., 2003). In fact, the THg measured in F3 exceeded 50 μg L^{-1} in almost all the samples. However, the presence of Hg^0 was not completely supported by experimental evidence due to lack of liquid Hg^0 balls (Bloom et al., 2003). THg-F5 was the second most abundant fraction in the analyzed samples (Fig. 3a). According to Bloom et al. (2003), Hg in this phase is mainly associated with mercuric sulphides such as cinnabar (HgS).

3.1.2 Microbiological characterization

Estimations of the total bacteria (DAPI count) in S_A and S_B exhibited values of 2.9 x 10^6 cells g^{-1} and 5.8 x 10^6 cells g^{-1}, respectively (Tab. 2). Data related to the heterotrophic and oil-degrading cultivable bacteria (CFU) and MPN method are shown in Table 2. A total of 200 randomly-picked clones containing 16S crDNA inserts were sequenced and their phylogenetic affiliation was determined. No chimeric sequences were detected among the clones. Sequences that were >97% similar were considered to have the same phylotype or operational taxonomic units (OTUs). A total of 21 different phylotypes (7 for S_A, 16 for S_B) were discerned, with each consisting of either a unique clone or a group of clones (Fig. 4). On the basis of the 16S crDNA clone library, the most prominent bacteria groups detected in S_A were Alpha-Proteobacteria (~45%) and Gamma-Proteobacteria (~20%) and Flavobacteria (~10%) in terms of the absolute number of clones and diversity of their sequences (Fig. 4a). Most of the population in S_B consisted of Gamma-Proteobacteria (~85%) and Epsilon-Proteobacteria (~10%) (Fig. 4a). A taxonomic analysis revealed that S_A was characterized by the presence of bacteria belonging to the genera *Sulfurovum* (ε-Proteobacteria; 44%; Inagaki et al., 2004) and *Thioalkalispira* (γ-Proteobacteria, order Chromatiales; 27%; Sorokin et al., 2002). On the other hand, *Thioalkalispira* was the dominant microbial population in S_B, which was the more contaminated sample (43%; Fig. 4b).

The *Thioalkalispira* and *Sulfurovum* genera belonged to the great group of SOB (Sorokin et al., 2011), which are commonly associated with environments rich in reduced sulfur compounds (S^{2-}, HS^-, H_2S, $S_2O_3^{2}$), such as hydrothermal vents or areas contaminated by industrial waste (Muyzer et al. 2013; Sorokin et al., 2011). Evidence for the common occurrence of SOB in marine sediments is accumulating, and it is also recognized that they play an important role in anaerobic sulphide oxidation (Brinkhoff et al., 1998; Brinkhoff and Muyzer, 1997; Sievert et al., 2000). Specifically, *Thioalkalispira* are extremophile bacteria indicative of strongly alkaline environments (pH=8÷10) (Sorokin et al., 2002). Herein, the peculiar presence of *Thioalkalispira* in both samples (S_A and S_B) could be an effect of contamination. Indeed, the brine purification waste from the chlor-alkali plant generally consisted of extremely alkaline sludge enriched in Hg (Basu et al., 2013; Sedivy, 2009).

3.2. Pore water

The levels of DHg in the pore water varied between 8.43 and 89.4 ng L^{-1} and 53.7 and 226 ng L^{-1} in cores 8 and 16, respectively (Fig. 2). In Core 8, DHg concentrations showed a downwards increasing trend, with pronounced enrichment in the 11-15 cm interval (up to 89.4 ng L^{-1}, Fig. 2). Thereafter, the DHg values decreased with depth (Fig. 2). Core 16 had the highest DHg values,

which exhibited wide variability, with two evident peaks at 0.5 cm (146 ng L^{-1}) and 5.5 cm (226 ng L^{-1}) (Fig. 2). After the maximum recorded at 5.5 cm, the DHg slightly decreased but the values remained elevated in the 7.5-17 cm interval (Fig. 2). The sediment-pore water distribution coefficient, THg log K_d (L/kg), was calculated as the ratio between the Hg in the sediment (THg_{sed}) and the pore water (DHg) (Marvin-DiPasquale et al., 2009). The THg log K_d had values in the intervals 4.8÷5.8 (Core 8) and 1.8÷2.5 (Core 16) (Fig. 2).

The depth profiles of dissolved Fe (Fe_{pw}), Mn (Mn_{pw}) and [SO_4^{-2}] in the pore water are shown in Figure 5. In Core 8, the Fe_{pw} (1.97÷81.0 μmol L^{-1}) began to increase at 6.5 cm, with the maximum value of 81 μmol L^{-1} documented at 13 cm, after which the levels decreased down to 25.5 μmol L^{-1} (at 17 cm). Concentrations then increased with depth (Fig. 5). The Mn_{pw} (0.15÷10.0 μmol L^{-1}) values slightly increased at 2.5-6.5, after which they increased steeply up to 6.45 μmol L^{-1} and then slowly rose to average values of 8 μmol L^{-1} (Fig. 5). [SO_4^{-2}] (32.6÷48.8 mmol L^{-1}) abruptly declined in the uppermost 1.5 cm, and then gradually increased with depth, except for two sharp falls at 11-13 cm and 17 cm (Fig. 5). In Core 16, the Fe_{pw} (1.59÷44.1 μmol L^{-1}) levels began to increase at 2.5 cm and the highest values were found at 4.5-9.5 cm. Concentrations then fell with depth (Fig. 5). Similarly, the Mn_{pw} (0.09÷5.52 μmol L^{-1}) values started to increase at 1.5 cm and were highest at 4.5-9.5 cm (Fig. 5). These levels then decreased with depth (Fig. 5). [SO_4^{-2}] (30.4÷52.0 mmol L^{-1}) rapidly declined in the uppermost 3.5 cm and remained low at 3.5-6.5 cm, after which the concentrations increased at 7.5-11 cm and then irregularly dropped off with depth (Fig. 5).

4. Discussion

The accumulation and distribution of Hg in sediment strictly depend on the nature of the transfer and the biogeochemical transformations taking place at the sediment-seawater interface and within the sediment itself. Natural organic matter is an important scavenger for Hg, because of the formation of strong bonds between Hg and functional groups such as thiol (R-SH), disulphide (R-SS-R) and disulphane (R-SSH) (e.g., Xia et al., 1999). In this way, Hg can be adsorbed to particulate organic matter along the water column and, ultimately, sequestered into sediment (Ravichandran, 2004). This mechanism is generally well supported by strong positive correlations between Hg and the organic matter documented in marine sediment (e.g., Conaway et al., 2003; Gagnon et al., 1997; Hammerschmidt et al., 2004; Hammerschmidt and Fitzgerald, 2004, 2006; Heyes et al., 2006; Sunderland et al., 2006). In the Augusta sediments, the relationship between THg and TOC is weak (Fig. 6). This, together with the indication of low amounts of THg-F3 (Fig.

3a) suggests that organic matter represents a minor control on the distribution of THg in this environment. This is typical of polluted areas, where inputs of large amounts of anthropogenic Hg cause considerable disproportion with organic matter in the sediment (Beldowski et al., 2014; Benoit et al., 2006; Covelli et al., 2009; Mason and Lawerence, 1999). Specifically, the Hg inputs in the Augusta sediments were mainly controlled by an anthropogenic source associated with brine purification waste from the chlor-alkali plant (Croudace et al. 2015), which contained large amounts of free elemental Hg (Hg^0; Sedivy, 2009). This could justify the SSE results, with major contents of THg-F4 (Fig. 3a) with Hg^0 reported to be the predominant solid-phase component in this extraction step (Bloom et al., 2003). THg-F4 can also contain Hg linked to Fe oxides such as hematite (α-Fe_2O_3), which is widely found in the Augusta sediments (Tab. 2). Nevertheless, the lack of correlation between THg and the hematite contents in the bulk samples does not enable us to prove this sort of association definitively. Orecchio and Polizzoto (2013) documented minor fractions of Hg linked to Fe-Mn oxides. Another important percentage of THg in the Augusta sediments appears to be associated with sulphides (THg-F5, Fig. 3a-b). In sulphuric anoxic sediments the formation of cinnabar (HgS), as well as metal-sulphides, is easily promoted by sulphate reduction activity, as originally suggested by Revis et al. (1989). However, we do not exclude the possibility that Hg could be co-precipitated as mixed sulphides (HgFeS) or adsorbed to surface functional groups of FeS (Jeong and Hayes, 2003; Wolfenden et al., 2005). Strong complexed forms (Hg-F4) and HgS synthesize the Hg solid-phases that control the THg in the Augusta sediments (Fig. 3b) and their geochemical behaviour plays a key role in the re-mobilization of Hg during different phases of *early diagenesis*.

4.1. Diagenesis of mercury in the Augusta Bay sediments

The depth profiles of Fe_{pw}, Mn_{pw} and $[SO_4^{-2}]$ are proxies of redox reactions taking place within the sediment during processes of *early diagenesis* (e.g. Froelich et al., 1979). Steep decreases of $[SO_4^{-2}]$ in the uppermost centimeter of Augusta sediments (0-4 cm) clearly reflect the process of sulphate reduction (Fig. 5). Concurrently, the increasing trend of the pyrite (FeS_2) content (Fig. 5) suggests high activity of H_2S and polysulphides ($H_xS_n^{x-2}$, x=0-2), which are essential reactants in the pathway for pyrite formation at low temperatures (Berner, 1970; Luther, 1991; Rickard, 1975; Rickard and Luther, 1997, 2007; Rickard and Morse, 2005; Schoonen and Barnes, 1991). The Mn-Fe reduction zone occurs 2-6 cm below the top of the sediment, where the sulphate reduction is already active (Fig. 5). According to modern views of *early diagenesis* (e.g., Aller, 1994; Fossing et al., 2000; Postma and Jakobsen, 1996;), it is evident that there is an overlapping of the biogeochemical zones that proceed simultaneously in a spatially and temporally complex sequence

within the sediment (Fig. 5). Furthermore, increases in [SO_4^{-2}] close to the Mn-Fe reduction zone suggest mechanisms in which the regeneration of [SO_4^{-2}] could be favoured (Fig. 5). The renewal of sulphate can be the result of the sulphide oxidation that is typically active in the suboxic-anoxic zone in marine sediment (Holmkvist et al., 2011; Luther et al., 1986). In fact, the H_2S generated by sulphate reduction will react spontaneously with Fe-Mn oxide, as expected by following equations:

$$3H_2S + 2FeOOH \rightarrow S^0 + 2FeS + 4H_2O \quad (1)$$

$$H_2S + MnO_2 \rightarrow S^0 + Mn^{2+} + 2OH^- \quad (2)$$

The formed S^0 can subsequently be reduced again to H_2S and oxidized to SO_4^{2-} by microbial activity (Thamdrup et al. 1993), as synthetically reported in the equation below:

$$S^0 + 4H_2O \rightarrow 3H_2S + SO_4^{2-} + 2H^+ \quad (3)$$

The combinations of a spontaneous sulphide oxidation (equations 1 and 2) and a microbial catalyzed disproportionation (equations 3) describe the overall reactions of disproportionation of zero-valent sulfur (S^0) coupled to Fe and Mn reduction (Thamdrup et al. 1993):

$$3S^0 + 2FeOOH \rightarrow SO_4^{2-} + 2FeS + 2H^+ \quad (4)$$

$$S^0 + 3MnO_2 + H_2O \rightarrow SO_4^{2-} + Mn^{2+} + 4OH^- \quad (5)$$

These reactions provides an explanation for mechanisms of sulphide oxidation in the presence of Fe-Mn (Terminal Electron Acceptor, TEA) in anoxic sediment. Coherently, significant amounts of S^0 are frequently found in the Mn-Fe redox zone (suboxic zone) of coastal marine sediment (Burdige and Nealson, 1986; Pyzik and Sommer, 1981; Sørensen and Jørgensen, 1987; Thode-Andersen and Jørgensen, 1989; Troelsen and Jørgensen, 1982;) where disproportionating bacteria occur abundantly (Canfield and Thamdrup, 1996; Finster et al., 1998; Thamdrup et al. 1993). Oxidative sulphide reactions (4) and (5) plausibly take place in the Augusta sediments. Observable evidence is the increase in sulphate in the Fe-Mn zone that is related to evidence of disseminated precipitation of pyrite (Fig. 5). Moreover, the existence of SOB (Tab. 4) suggests the presence of S^0, which is an essential substrate for growth of *Sulfurovum* and *Thioalkalispira* (Inagaki et al., 2004; Sorokin, 2002). Noteworthy, the microbial respiration of *Thioalkalispira* occurs due to the effect of sulphide oxidation via polysulphide and elemental sulfur oxidation to sulphate (Sorokin et al., 2002). These findings suggest that *Sulfurovum* and *Thioalkalispira* are adapted to live in the presence of high concentrations of Hg and we suggest that they play a functional role of suphide oxidizer in re-cycling sulfur in the Augusta sediments. Accordingly, the biogeochemical zones appear to be driven by the microbial sulphate reduction in the uppermost sediment (0-4 cm) and by the Fe-Mn reduction probably associated with the oxidation of sulphide in the deeper part of the sediment (Fig. 7).

The maximum release of DHg occurs close to the Fe and Mn redox zone (Fig. 7), as also evidenced by correlations between Fe_{pw} and Mn_{pw} and DHg in the pore water (r=0.68 and r=0.78, $p<0.05$; n=15; for Fe and Mn respectively). The microbial dissolution of Fe-Mn oxides could be an explanation for the DHg enhancement in the pore water (Gagnon et al., 1996; Gagnon et al., 1997; Gobeil and Cossa, 1993; Guentzel et al, 1996; Quemerais et al., 1998) where most of the Hg solid-phase in the Augusta sediments consists of "immobile" forms like Hg^0 and HgS. Strong complexed forms associated with HgF4 are highly stable in sediments and species like the Hg^0 accounts for negligible amounts in pore water (Bouffard and Amyot, 2009). Therefore, in all likelihood, THg-F4 is not the main solid-phase controlling the patterns of DHg in the Augusta pore water. Also, in marine sediment, the occurrence of sulphides contributes to reductions in the affinity of Fe-Mn oxyhydroxides with Hg (Bono, 1997; Chakraborty et al., 2016; Dmytriw et al., 1994; Eganhouse, et al., 1978; Giordano et al., 1992; Matty and Long, 1995,).

It is commonly recognized that the mobility of HgS in sediment would be limited because of its very low solubility ($k_{ps}=10^{-36,8}$; Schwarzenbach and Widmer, 1963). For this reason, HgS is considered to be a sink of Hg in the sedimentary compartment. Nonetheless, HgS solubility can notably increase in anoxic conditions when the activity of sulphide is high (Benoit et al, 1999a; Paquette and Heltz, 1997, 1995). Figure 8 shows the predicted DHg curves generated by the pure cinnabar solubility model, in which a rise of DHg with increasing sulphide concentrations is evident (Benoit et al, 1999a). In this model, the value of K_{sp} determines the maximum DHg at high sulphide levels, while the minimum value of DHg at low sulphide levels is given by the $K_{s1}=10^{-10}$, value proposed by Dyrssen and Wedborg (1991, 1989). Once typical dissolved sulphide concentrations for anoxic sediment are considered (from 1μM to 1mM; Rickard and Morse, 2005), the average values of DHg for cores 8 and 16 exhibit an order of magnitude comparable to those expected by HgS dissolution (Fig. 8). Moreover, the DHg of the A and B samples (Tab. 3), for which the concentration of sulphide ~3mM (culture sulphide level for SOB; Sorokin et al, 2002) has been considered, falls very close to the pure cinnabar solubility curve (Fig. 8). Therefore, the dissolution of HgS is a reasonable explanation for the patterns of DHg in the pore water of the Augusta sediments. The theoretical modelling of Hg partitioning between the solid and aqueous phases in sediments emphasise the fact that log K_d can fall when soluble Hg-sulphides and polysulphides are formed in solution (Skyllberg, 2008; 2012). Therefore, we speculate that the average values of the THg log K_d, which are equivalent to 5.2 (Core 8) and 2.2 (Core 16), could suggest equilibrium between the sediment and pore water in the presence of polysulphides. Similar values were reported for other anoxic sediments where polysulphide production was expected (3.5÷4.5 L Kg^{-1}; Goulet et al., 2007; Hammerschmidt and Fitzgerald, 2004; Hurley et al., 1994; Schartup et al., 2014).

Polysulphides can form as byproducts in the microbial oxidation of sulphide (e.g., *Thioalkalispira* respiration pathway), and also in the dispropotionation reactions (4) and (5), when elemental sulphur (S^0) reacts with sulphides (Roy and Trudinger, 1970). We hypothesize that the oxidative pathways of sulphide, probably carried out by *Thioalkalispira*, close to the Fe-Mn redox zone created conditions of high S^0 activity, which promoted the generation of polysulphides in the Augusta sediments. Consequently, the HgS solubility increased by the following way (Paquette and Heltz, 1997):

$$(n\text{-}1)\ S^0 + xH^+ + yHS^- + HgS(cinn) \leftrightarrow Hg(S_n)(SH)^- \text{ (mercury polysulphide)} \quad (6)$$

Over a broad, near neutral, pH range, $Hg(S_n)(SH)^-$ is the predominant Hg(II) complex in solutions saturated with S^0 (Paquette and Heltz, 1997). We do not have information on the concentrations of S^0 or polysulphides in the pore water, but we do have evidence that active bacteria like *Thioalkalispira* grow in the sediment and are able to produce polysulphides (Sorokin et al., 2002). Furthermore, the presence of pyrite is a clear signal of polysulphide activity in the Augusta sediments (Berner, 1970; Rickard, 1975). These evidence suggest Fe and Mn to be important oxidants for reduced sulphur compounds in anoxic sediments. It is reasonable to hypothesize that anaerobic sulphide oxidation coupled to Fe-Mn reduction can be considered an important factor affecting metal-sulphides dissolution, such as HgS, with consequent re-mobilization of contaminant from coastal marine sediments. Furthermore, the sequence of biogeochemical zone in the Augusta sediments (Fig. 7) represents a diagenetic environment in which the presence of reduced layers near the sediment-seawater interface (0-4 cm, Fig. 7) facilitate the diffusion of Hg from the Mn-Fe reduction zones directly to the overlying water column.

5. Conclusion

The results of this study demonstrate that free elemental mercury (Hg^0), probably associated with waste from a chlor-alkali plant, and mercury sulphides such as cinnabar (HgS), dominate the mercury association in the Augusta sediment. However, although the sedimentary Hg is predominantly associated with "immobile" forms, documented high DHg levels were interpreted as being strictly related to the effects of Fe and Mn redox dynamics associated with sulphide oxidation in the deeper sediment. The generation of polysulphides, as intermediate compounds for sulphides oxidation, could favour chemical conditions for high Hg mobility. Specifically, an increase in HgS solubility in the presence of polysulphides is considered to be the key mechanism affecting the diagenesis of Hg in the sediment. *Thioalkalispira* sulphur oxidizing bacteria, which are able to

produce polysulphides during their respiration processes, indirectly support HgS dissolution and, consequently, the release of Hg from the Augusta Bay sediments. Therefore, the enrichment of *Thioalkalispira* in the more contaminated sample suggests that these bacteria have a specific and crucial biogeochemical role in processes of Hg detoxificationas sulphide oxidizer and re-cycler of sulfur in the Augusta sediments.

Acknowledgements

Funding for this study was provided by the Regional Health Department of Syracuse (Sicily). The authors wish to thank the crew of R/V *L. Dalla Porta* for their valuable professionalism and support during the oceanographic cruise. We are grateful to Dr. L. Giaramita (IAMC-CNR, Capo Granitola) and V. Tancredi (IAMC-CNR, Capo Granitola) for their laboratory assistance. Thanks are also due to the personnel of the port authorities of Augusta town and Dr. F. Bulfamante (IAMC-CNR, Capo Granitola) for their precious logistic support for all the research activities realized in the field.

Reference

Aller, R.C., 1994. Bioturbation and remineralization of sedimentary organic matter: effects of redox oscillation. Chem. Geol. 114, 331–345.

American Public Health Association (APHA), 1992. Standard Methods for the Examination of Water and Waste Water, eighteenth ed. Washington, DC.

Barahona, E., Huertas, F., Pozzuoli, A., Linares, J., 1982. Mineralogia e genesi dei sedimenti della provincia di Granata (Spagna). Acta Mineral. Petrogr. 26, 61–90.

Barkay, T., Wagner-Döbler, I., 2005. Microbial transformations of mercury: Potentials, challenges, and achievements in controlling mercury toxicity in the environment. Adv. Appl. Microbiol. 57, 1–52.

Basu, S., Mukhopadhyay, S.K., Gangopadhyay, A., Dastidar, S.G., 2013. Characteristic Change of Effluent from a Chlor-alkali Industry of India due to Process Modification. Int. Res. J. Environment Sci. 2, 44–47.

Bełdowski, J., Miotk, M., Bełdowska, M., Pempkowiak, J., 2014. Total, methyl and organic mercury in sediments of the Southern Baltic Sea. Mar. Pollut. Bull. 87, 388–395.

Bellucci, L.G., Giuliani, S., Romano, S., Albertazzi, S., Mugnai, C., Frignani, M., 2012. An integrated approach to the assessment of pollutant delivery chronologies to impacted areas: Hg in the augusta bay (Italy). Environ. Sci. Technol. 46, 2040–2046.

Benoit, J.M., Gilmour, C.C., Mason, R.P., Heyes, A., 1999a. Sulfide controls on mercury speciation and bioavailability to methylating bacteria in sediment pore water. Environ. Sci. Technol. 33, 951–957.

Benoit, J.M., Mason, R.P., Gilmour, C.C., 1999b. Estimation of mercury-sulfide speciation in sediment pore waters using octanol-water partitioning and implications for availability to methylating bacteria. Environ. Toxicol. Chem. 18, 2138–2141.

Benoit, J.M, Gilmour C.C., Mason, R.P., 2001a. Aspects of bioavailability of mercury for methylation in pure cultures of Desulfobulbus propionicus (1pr3). Appl. Environ. Microb. 67, 51–58.

Benoit, J.M., Mason, R.P., Gilmour, C.C., 2001b. The influence of sulfide on solid-phase mercury bioavailability for methylation by pure cultures of Desulfobulbus propionicus (1pr3). Environ. Sci. Technol. 35, 127–132.

Benoit, J.M., Shull, D.H., Robinson, P., Ucran, L.R., 2006. Infaunal burrow densities and sediment

monomethyl mercury distributions in Boston Harbor, Massachusetts. Mar. Chem. 102, 124–133.

Berner, R.A., 1970. Sedimentary Pyrite Formation. Am. J. Sci. 268, 1–23.

Bloom, N.S., Preus, E., Katon, J., Hiltner, M., 2003. Selective extractions to assess the biogeochemically relevant fractionation of inorganic mercury in sediments and soils. Anal. Chim. Acta 479, 233–248.

Bono, A., 1997. The partitioning of mercury in the solid components of sediment of the Saguenay fjord, Quebec. M.S. Thesis, McGill Univ. Montr.

Bonsignore, M., Salvagio Manta, D., Oliveri, E., Sprovieri, M., Basilone, G., Bonanno, A., Falco, F., Traina, A., Mazzola, S., 2013. Mercury in fishes from Augusta Bay (southern Italy): Risk assessment and health implication. Food Chem. Toxicol. 56, 184–194.

Bonsignore, M., Tamburrino, S., Oliveri, E., Marchetti, A., Durante, C., Berni, A., Quinci, E., Sprovieri, M., 2015. Tracing mercury pathways in Augusta Bay (southern Italy) by total concentration and isotope determination. Environ. Pollut. 205, 178–85. doi:10.1016/j.envpol.2015.05.033

Bothner, M.H., Jahnke, R.A., Peterson, M.L., Carpenter, R., 1980. Rate of mercury loss from contaminated estuarine sediments. Geochim. Cosmochim. Acta 44, 273–285.

Bouffard, A., Amyot, M., 2009. Importance of elemental mercury in lake sediments. Chemosphere 74, 1098–1103.

Brinkhoff, T., Muyzer, G., 1997. Increased species diversity and extended habitat range of sulfur- oxidizing Thiomicrospira spp. Appl. Environ. Microbiol. 63, 3789–3796.

Brinkhoff, T., Santegoeds, C.M., Sahm, K., Kuever, J., Muyzer, G., 1998. A Polyphasic Approach To Study the Diversity and Vertical Distribution of Sulfur-Oxidizing Thiomicrospira Species in Coastal Sediments of the 64, 4650–4657.

Burdige, D.J., Nealson, K. H., 1986. Chemical and microbiological studies of sulfide-mediated manganese reduction. Geochem. J. 4, 361–387.

Canfield, D. E., Thamdrup B. 1996. Fate of elemental sulfur in an intertidal sediment. FEMS Microb. Ecol. 19, 95–103.

Cappello, S., Caruso, G., Zampino, D., Monticelli, L.S., Maimone, G., Denaro, R., Tripodo, B., Troussellier, M., Yakimov, M., Giuliano, L., 2007. Microbial community dynamics during assays of harbour oil spill bioremediation: A microscale simulation study. J. Appl. Microbiol. 102, 184–194.

Chakraborty, P., Vudamala, K., Chennuri, K., Armoury, K., Linsy, P., Ramteke,D, Sebastian, T., Jayachandran, S., Naik, C., Naik, R., Nath, B.N., 2016. Mercury profiles in sediemnt from the marginal high of Arabian Sea: an indicator of increasing anthropogenic Hg input. Environ. Sci. Pollut. Res. 23, 8529-8538.

Chatziefthimiou, A.D., Crespo-Medina, M., Wang, Y., Vetriani, C., Barkay, T., 2007. The isolation and initial characterization of mercury resistant chemolithotrophic thermophilic bacteria from mercury rich geothermal springs. Extremophiles 11, 469–479.

Compeau, G.C., Bartha, R., 1985. Sulfate-reducing bacteria: Principal methylators of mercury in anoxic estuarine sediment. Appl. Environ. Microbiol. 50, 498–502.

Conaway, C.H., Squire, S., Mason, R.P., Flegal, A.R., 2003. Mercury speciation in the San Francisco Bay estuary. Mar. Chem. 80, 199-225.

Cossa, D., Gobeil, C., 2000. Mercury speciation in the Lower St. Lawrence Estuary. Can. J. Fish. Aquat. Sci. 57, 138–147.

Covelli, S., Acquavita, A., Piani, R., Predonzani, S., De Vittor, C., 2009. Recent contamination of mercury in an estuarine environment (Marano lagoon, Northern Adriatic, Italy). Estuar. Coast. Shelf Sci. 82, 273–284.

Covelli, S., Emili, A., Acquavita, A., Koron, N., Faganeli, J., 2011. Benthic biogeochemical cycling of mercury in two contaminated northern Adriatic coastal lagoons. Cont. Shelf Res. 31, 1777–1789.

Croudace I.W., Romano, E., Ausili, A., Bergamin, L., Rothwell., R.G., 2015. X-Ray Core Scanners as an Environmental Forensics Tool: A Case Study of Polluted Harbour Sediment (Augusta Bay, Sicily), in: Croudace, I.W., Rothwell, R.G. (Eds.), Micro-XRF Studies of Sediment Cores, Developments in Paleoenvironmental Research 17. Springer Science+Business Media Dordrecht, pp.393-420.

Dmytriw, R., Mucci, A., Lucotte, M., Pichet, P., 1994. The partitioning of mercury in the solid components of pristine and flooded forest soils and sediments from a hydroelectric reservoir, Québec, (Canada). Wat. Air Soi1 Poll. 80, 1099-1103.

Dyksterhouse, S.E., Gray, J.P., Herwig, R.P., Lara, J.C., Staley, J.T., 1995. Cycloclasticus pugetii gen. nov., sp. nov., an aromatic hydrocarbon-degrading bacterium from marine sediments. Int. J. Syst. Bacteriol. 45, 116–123.

Dyrssen, D., Wedborg, M., 1991. The sulphur mercury-II system in natural waters. Water Air Soil Pollut. 56, 507-20

Dyrssen, D., Wedborg, M., 1989. The state of dissolved trace sulphide in seawater. Mar. Chem. 26,289–293.

Eganhouse, R.P., Young, D.R., Johnson, J.N., 1978. Geochemistry of mercury in Palos Verde Sediments. Env. Sci. Tech. 12, 1151 - 1157.

Feyte, S., Tessier, A., Gobeil, C., Cossa, D., In situ adsorption of mercury, methylmercury and other elements by iron oxyhydroxides and organic matter in lake sediments. Appl. Geochem. 25, 984-995.

Fergusson, J.E., 1990. The Heavy Elements: Chemistry, Environmental Impact and Health Effects, firts ed Pergamon Press, Oxford, England.

under anaerobic conditions. Nature 346, 742–744.

Finster, K., Liesack, W., Thamdrup, B., 1998. Elemental sulfur and thiosulfate disproportionation by Desulfocapsa sulfoexigens sp. nov., a new anaerobic bacterium isolated from marine surface sediment. Appl. Environ. Microbiol. 64, 119–125.

Fitzgerald, W.F., Lamborg, C.H., Hammerschmidt, C.R., 2007. Marine Biogeochemical Cycling of Mercury. Chem. Rev. 107, 641–662.

Fossing, H., Ferdelman, T.G., Berg, P. 2000. Sulfate reduction and methane oxidation in continental margin sediments influenced by irrigation (South-East Atlantic off Namibia). Geochim. Cosmochim. Acta 64, 897–910.

Froelich, P.M., Klinkhammer, G.P., Bender, M.L., Lurdtke, N.A., Heath, G.R., Cullen, D., Dauphin, P., Hammond, D., Hartman, B., Maynard, V., 1979. Early oxidation of organic matter in pelagic sediments of the eastern equatorial Atlantic: suboxic diagenesis. Geochim. Cosmochim. Acta 43, 1075–1090.

Gagnon, C., Pelletier, E., Mucci, A., 1997. Behaviour of anthropogenic mercury in coastal marine sediments. Mar. Chem. 59, 159–176.

Gilmour, C.C., Henry, E.A., Mitchell, R., 1992. Sulfate stimulation of mercury methylation in freshwater sediments. Environ. Sci. Technol. 26, 2281–2287.

Giordano, R., Musmeci, L., Ciaralli, L., Venillo, I., Chiraco, M., Piccioni, A., Costantini, S., 1992. Total contents and sequential extractions of mercury, cadmium, and lead in coastal sediments. Mar. Poll. Bull 24, 320-357.

Gobeil, C., Cossa, D., 1993. Mercury in sediments and sediment porewater in the Laurentian through. Can. J. Fish. Aquat. Sci. 50, 1794–1800.

Goulet, R., Holmes, J., Page, B., Poissant, L., Siciliano, S.D., Lean, D.R.S., Wang, F., Amyot, M., Tessier, A., 2007. Mercury transformations and fluxes in sediments of a riverine wetland. Geochim. Cosmochim. Acta 71, 3393–3406.

Guentzel, J.L., Powell, R.T., Landing, W.M., Mason, R.P., 1996. Mercury associated with colloidal material in an estuarine and an open- ocean environment. Mar. Chem. 55, 177–188.

Hammerschmidt, C.R., Fitzgerald, W.F., 2006. Methylmercury cycling in sediments on the continental shelf of southern New England. Geochim. Cosmochim. Acta 70, 918–930.

Hammerschmidt, C.R., Fitzgerald, W.F., 2004. Geochemical Controls on the Production and Distribution of Methylmercury in Near-Shore Marine Sediments. Environ. Sci. Technol. 38, 1487–1495.

Hammerschmidt, C.R., Fitzgerald, W.F., Lamborg, C.H., Balcom, P.H., Visscher, P.T., 2004. Biogeochemistry of methylmercury in sediments of Long Island Sound. Mar. Chem. 90, 31–52.

Heyes, A., Mason, R.P., Kim, E., Sunderland, E., 2006. Mercury methylation in estuaries: insights from using measuring rates using stable mercury isotopes. Mar. Chem. 102, 134-147.

Holmkvist, L., Ferdelman, T.G., Jørgensen, B.B., 2011. A cryptic sulfur cycle driven by iron in the methane zone of marine sediment (Aarhus Bay, Denmark). Geochim. Cosmochim. Acta 75, 3581–3599.

Huerta-Diaz, M.A., Morse, J.W., 1992. Pyritization of trace metals in anoxic marine sediments. Geochim. Cosmochim. Acta 56, 2681–2702.

Hurley, J. P ., Krabbenhoft, D. P., Babiarz , C. L., Andren, A. W., 1994. Cycling of mercury across the sediment-water interface in seepage lakes, in: Baker, L. A. (Ed), Environmental Chemistry of Lakes and Reservoirs. Advances in Chemistry Series, 237. American Chemical Society, Washington, DC, pp. 425-449.

ICRAM, 2008. Istituto Centrale Per La Ricerca Scientifica E Tecnologica Applicata Al Mare, Progetto preliminare di bonifica dei fondali della rada di Augusta nel sito di interesse nazionale di Priolo – Elaborazione definitiva, BoI-Pr-SI-PR-Rada di Augusta-03.22, pp. 182.

Inagaki, F., Takai, K., Nealson, K.H., Horikoshi, K., 2004. Sulfurovum lithotrophicum gen. nov., sp. nov., a novel sulfur-oxidizing chemolithoautotroph within the E-Proteobacteria isolated from Okinawa Trough

hydrothermal sediments. Int. J. Syst. Evol. Microbiol. 54, 1477–1482.

Jay, J. A., Morel, F.M.M., Hemond, H.F., 2000. Mercury speciation in the presence of polysulfides. Environ. Sci. Technol. 34, 2196-2200.

Jeong, H.Y., Hayes, K.F., 2003. Impact of transition metals on reductive dechlorination rate of hexachloroethane by mackinawite. Environ. Sci. Technol. 37, 4650–4655.

Jonsson, S., Skyllberg, U., Nilsson, M.B., Lundberg, E., Andersson, A., Björn, E., 2014. Differntiated availability of geochemical mercury pools controls methymercury levels in estuarine sediemnt and biota. Nat. Commun.5, doi: 10.1038/ncomms5624.

King, J.K., Kostka, J.E., Frischer, M.E., Saunders, F.M., 2000. Sulfate- reducing bacteria methylate mercury at variable rates in pure culture and in marine sediments. Appl. Environ. Microb. 66, 2430–2437.

Kuwae, T., Hosokawa, Y., 1999. Determination of abundance and biovolume of bacteria in sediments by dual staining with 4',6-diamidino-2-phenylindole and acridine orange: Relationship to dispersion treatment and sediment characteristics. Appl. Environ. Microbiol. 65, 3407–3412.

Lane, D.J., 1991. 16/23S rRNA sequencing, in: Stackerbrandt, E., Goodfellow, M. (Eds.), Nucleic acid techniques in bacterial systematics. Wiley, New York, pp. 115-175.

Luther, G.W., 1991. Pyrite synthesis via polysulfide compounds. Geochim. Cosmochim. Acta 55, 2839–2849.

Luther, G.W., Church, T.M., Giblin, A.E., Howarth, R.W., 1986. Speciation of dissolved sulfur in salt marshes by polarographic methods. Org. Mar. Geochem. 305, 340–355.

Marvin-Dipasquale, M., Lutz, M.A., Brigham, M.E., Krabbenhoft, P., Aiken, G.R., Orem, W.H., Hall, B.D., Krabbenhoft, D.P., 2009. Mercury Cycling in Stream Ecosystems. 2. Benthic Methylmercury Production and Bed Sediment-Pore Water Partitioning. Environ. Sci. Technol. 43, 2726–2732.

Mason, R., Bloom, N., Cappellino, S., Gill, G., Benoit, J., 1998. Investigation of porewater sampling methods for mercury and methylmercury. Environ. Sci. Technol. 32, 4031–4040.

Mason, R.P., Lawrence, A.L., 1999. Concentration, distribution, and bioavailability of mercury and methylmercury in sediments of Baltimore Harbor and Chesapeake Bay, Maryland, USA. Environ. Toxicol. Chem. 18, 2438-2447.

Matty, J.M., Long, D.T., 1995. Early diagenesis of mercury in the Laurentian Great Lakes. J. Great Lakes

Res. 21, 574-586.

Muyzer, G., Kuenen J.G., Robertson L.A., 2013. Colorless Sulfur Bacteria, in: Rosenberg, E., DeLong E.F., Lory, S., Stackebrandt, E., Thompson F. (Eds.), The prokaryotes - Prokaryotic physiology and biochemistry. Springer-Verlag Berlin Heidelberg, pp. 555-588.

Nakanishi, H., Ukita, M., Sekine, M., Murakami, S., 1989. Mercury pollution in Tokuyama Bay. Hydrobiology 176/177, 197–211.

Orecchio, S., Polizzotto, G., 2013. Fractionation of mercury in sediments during draining of Augusta (Italy) coastal area by modified Tessier method. Microchem. J. 110, 452–457.

Paquette, K., Helz, G., 1995. Solubility of cinnabar (red HgS) and implications for mercury speciation in sulfidic waters. Water. Air. Soil Pollut. 80, 1053–1056.

Paquette, K.E., Helz, G.R., 1997. Inorganic speciation of mercury in sulfidic waters: The importance of zero-valent sulfur. Environ. Sci. Technol. 31, 2148–2153.

Pyzik, A.J., Sommer, S.E., 1981.Sedimentary iron monosulfides: kinetics and mechanism of formation. Geochim. Cosmochim. Acta 45,687-698.

Postma, D., Jakobsen, R., 1996. Redox zonation: Equilibrium constraints on the Fe(III)/SO_4^- reduction interface. Geochim. Cosmochim. Acta 60, 3169–3175.

Quemerais, B., Cossa, D., Rondeau, B., Pham, T. T., Fortin, B., 1998. Mercury distribution in relation to iron and manganese in the waters of the St. Lawrence River. Sci. Total Environ., 213, 193–201.

Ranchou-Peyruse, M., Monperrus, M., Bridou, R., Duran, R., Amouroux, D., Salvado, J.C., Guyoneaud, R., 2009. Overview of mercury methylation capacities among anaerobic bacteria including representatives of the sulphate-reducers: implications for environmental studies. Geomicrobiol. J. 26, 1–8.

Ravichandran, M., 2004. Interactions between mercury and dissolved organic matter - A review. Chemosphere 55, 319–331.

Revis, N.W., Osborne, T.R., Holdsworth, G., Hadden, C., 1989. Distribution of mercury species in soil from a mercury-contaminated site. Water. Air. Soil Pollut. 45, 105–113.

Rickard, D., 1975. Kinetics and mechanisms of pyrite formation at low temperatures. Am. J. Sci. 275, 636–652.

Rickard, D., Luther, G.W., 1997. Kinetics of pyrite formation by the H_2S oxidation of iron(II) monosulfide

in aqueous solutions between 25 and 125 degrees C: the mechanism. Geochim. Cosmochim. Acta 61, 135–147.

Rickard D, Luther G.W., 2007. Chemistry of iron sulfides. Chem. Rev. 107, 514–562.

Rickard, D., Morse, J.W., 2005. Acid volatile sulfide (AVS), Mar. Chem. 97, 141-197.

Roy, A.B, Trudinger, P.A., 1970. The Biochemistry of Inorganic Compounds of Sulfur. Cambridge University Press, Cambridge, UK.

Sedivy, V.M., 2009. Environmental Balance of Salt Production speaks in favour of Solar Saltworks. Glob. NEST J. 11, 41–48.

Schartup, A.T., Mason, P.R., Balcom, P.H., Hollweg, T.A., Chen, C.Y., 2013. Methylmercury production in estuarine sediments: role of organic matter. Environ. Sci. Technol. 47, 695-700.

Schartup, A.T., Balcom, P.H., Mason, P.R., 2014. Sediment-Porewater Partitioning, Total Sulfur, and Methylmercury Production in Estuaries. Environ. Sci. Technol. 48, 954-960.

Schultz, L.G., 1964. Quantitative Interpretations of Mineralogic Composition from X-ray and Chemical Data for the Pierre Shale, 391-C. US Geological Survey Professional Paper 1–31.

Schoonen, M.A.A., Barnes, H.L., 1991. Reactions forming pyrite and marcasite from solution: II. Via FeS precursors below 100 °C. Geochim. Cosmochim. Acta 55, 1505–1514.

Schwarzenbach, G, Widmer, M., 1963. Die loeslichkeit von metallsulfiden. I. Schwarzes queck- silbersulfid. Helv. Chim. Acta 46, 2613–2628.

Sievert, S.M., Kuever, J.A.N., Muyzer, G., Sievert, S.M., Kuever, J.A.N., 2000. Identification of 16S Ribosomal DNA-Defined Bacterial Populations at a Shallow Submarine Hydrothermal Vent near Milos Island (Greece). Appl. Environ. Microbiol. 66, 3102–3109.

Simbahan, J., Kurth, E., Schelert, J., Dillman, A., Moriyama, E., Jovanovich, S., Blum, P., 2005. Community analysis of a mercury hot spring supports occurrence of domain-specific forms of mercuric reductase. Appl. Environ. Microbiol. 71, 8836–8845.

Skyllberg, U., 2012. Chemical speciation of mercury in soil and sediment, in: Liu, G., Cai, Y., O'Driscoll N., Environmental Chemistry and Toxicology of Mercury, first ed. John Wiley & Sons, Inc., pp. 219–258.

Skyllberg, U., 2008. Competition among thiols and inorganic sulfides and polysulfides for Hg and MeHg in wetland soils and sediments under suboxic conditions: Illumination of controversies and implications

for MeHg net production. J. Geophys. Res. 113, 1–14.

Sorokin, D., Tourova, T., Kolganova, T., Sjollema, K. a, Kuenen, J.G., 2002. *Thioalkalispira microaerophila* gen. nov., sp. nov., a novel lithoautotrophic, sulfur oxidizing bacterium from a soda lake. Int. J. Syst. Evol. Microbiol. 52, 2175–2182.

Sorokin, D.Y., Kuenen, J.G., Muyzer, G., 2011. The microbial sulfur cycle at extremely haloalkaline conditions of soda lakes. Front. Microbiol. 2, 1-15.

Sørensen, J., Jørgensen, B.B., 1987. Early diagenesis in sediments from Danish coastal waters: microbial activity and Mn–Fe–S geochemistry. Geochim. Cosmochim. Acta 51, 1883–1890.

Sprovieri, M., Oliveri, E., Di Leonardo, R., Romano, E., Ausili, A., Gabellini, M., Barra, M., Tranchida, G., Bellanca, A., Neri, R., Budillon, F., Saggiomo, R., Mazzola, S., Saggiomo, V., 2011. The key role played by the Augusta basin (southern Italy) in the mercury contamination of the Mediterranean Sea. J. Environ. Monit. 13, 1753–1760.

Sunderland, E.M., Gobas, F.A.P.C., Branfireun, B.A., Heyes, A., 2006. Environmental controls on the speciation and distribution of mercury in coastal sediments. Mar. Chem. 102, 111–123.

Thamdrup, B., Finster, K., Hansen, J.W., Bak, F., 1993. Bacterial disproportionation of elemental sulfur coupled to chemical reduction of iron or manganese. Appl. Environ. Microbiol. 59, 101–108.

Thode-Anderson, S., Jørgensen, B.B., 1989. Sulfate reduction and the formation of 35S-labeled FeS, FeS_2 and S^0 in coastal marine sediments. Limnol. Oceanogr. 34, 793–806.

Troelsen, H., Jørgensen, B.B., 1982. Seasonal dynamics of elemental sulfur in two coastal sediments. Estuar. Coast. Shelf Sci. 15, 255–266.

Vetriani, C., Chew, Y.S., Miller, S.M., Coombs, J., Lutz, R. a, Barkay, T., 2005. Mercury Adaptation among Bacteria from a Deep-Sea Hydrothermal Vent Mercury Adaptation among Bacteria from a Deep-Sea Hydrothermal Vent. Appl. Environ. Microbiol. 71, 220–226.

Wolfenden, S., Charnock, J.M., Hilton, J., Livens, F.R., Vaughan, D.J., 2005. Sulfide species as a sink for mercury in lake sediments. Environ. Sci. Technol. 39, 6644–6648.

Xia, K., Skyllberg, U., Bleam, W.F., Bloom, P.R., Nater, E.A., Helmke, P.A., 1999. X-ray absorption spectroscopic evidence for the complexation of Hg(II) by reduced sulfur in soil humic substances. Env. Sci Technol 33, 257–261.

Yakimov, M.M., Cappello, S., Crisafi, E., Tursi, A., Savini, A., Corselli, C., Scarfi, S., Giuliano, L., 2006. Phylogenetic survey of metabolically active microbial communities associated with the deep-sea coral Lophelia pertusa from the Apulian plateau, Central Mediterranean Sea. Deep. Res. Part I Oceanogr. Res. Pap. 53, 62–75.

Yakimov, M.M., Denaro, R., Genovese, M., Cappello, S., D'Auria, G., Chernikova, T.N., Timmis, K.N., Golyshin, P.N., Giluliano, L., 2005. Natural microbial diversity in superficial sediments of Milazzo Harbor (Sicily) and community successions during microcosm enrichment with various hydrocarbons. Environ. Microbiol. 7, 1426–1441.

Zampino, D., Zaccone, R., La Ferla, R., 2004. Determination of living and active bacterioplankton: a comparison of methods. Chem. Ecol. 20, 411–422.

CAPTIONS

Fig. 1 a) Location map of the Augusta Bay; **b)** distribution map of total mercury (THg) in bottom sediments with sampling sites in the Augusta harbour.

Fig. 2 Depth distribution of total organic carbon (TOC), total mercury (THg) in sediments, dissolved mercury (DHg) in sediment pore waters and THg log K_d for the Augusta cores.

Fig. 3 a) Partitioning of Hg in the solid phase of the Augusta sediments according to the selective extraction procedure **b)** relationship between THg in bulk sediments and THg in fractions F4 and F5.

Fig. 4 The structure of the microbial population determined using a taxonomic analysis (cloning library of 16S crDNA) for the Augusta samples.

Fig. 5 Depth distribution of dissolved Mn, Fe, SO_4^{2-} in sediment pore waters and pyrite content in sediments for the Augusta cores.

Fig. 6 Relationship between total organic carbon TOC and THg concentrations in the Augusta sediments.

Fig. 7 Schematic representation of sediment pore water profiles for the Augusta cores. The disproportionation of S^0 coupled to Fe and Mn reduction can explain some observations of the early diagenesis in the Augusta sediments (see text for details).

Fig. 8 Predicted curves of dissolved mercury (DHg) as function of sulphide concentration calculated using the cinnabar solubility model in the presence of excess cinnabar (from Benoit et al., 1999a). The square symbols are the average values of DHg in sediment pore waters of cores 8 and 16. The circle symbols are the DHg in sediment pore waters of the A and B samples (see text for details).

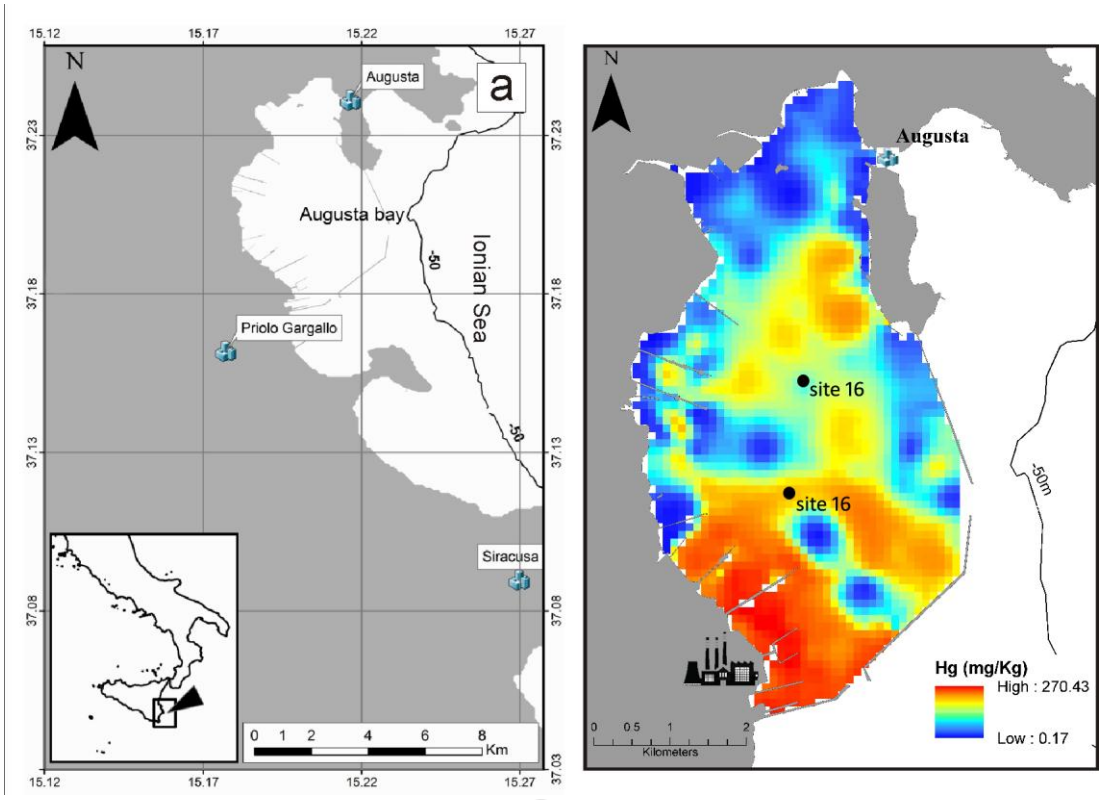

Figure 1

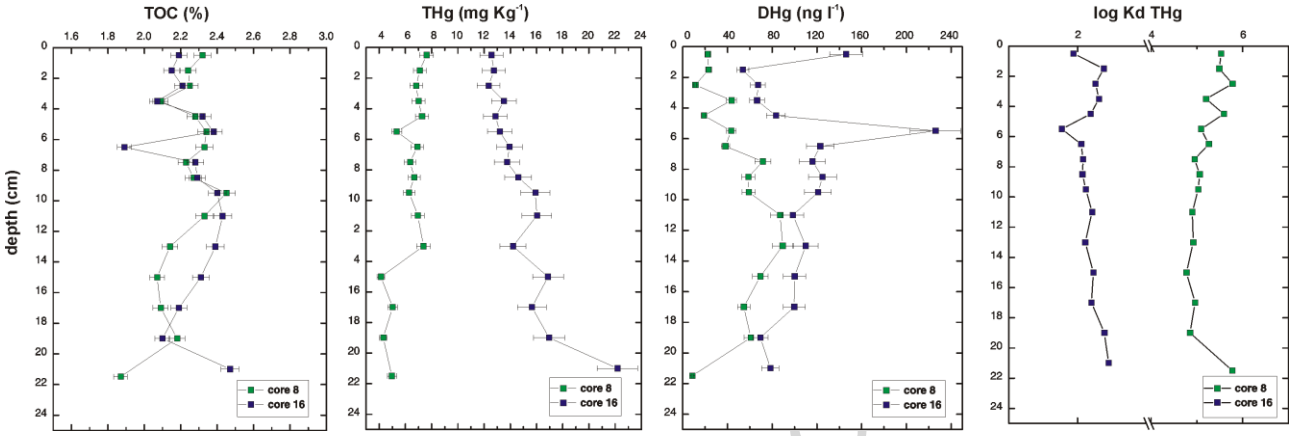

Figure 2

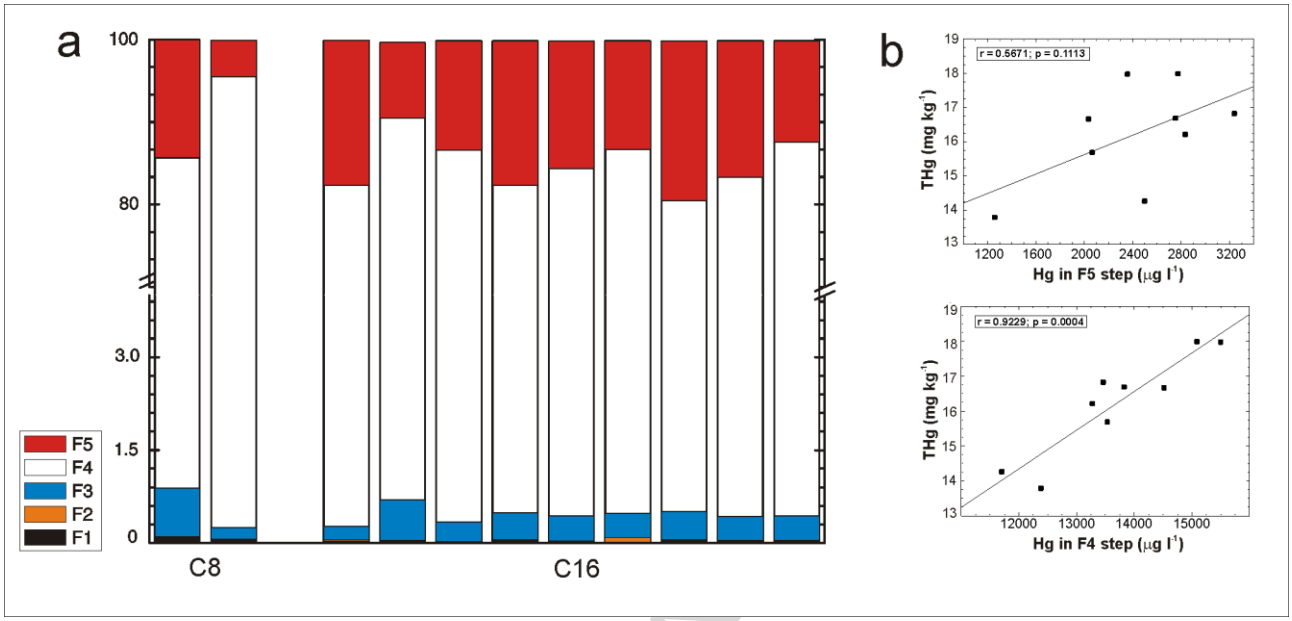

Figure 3

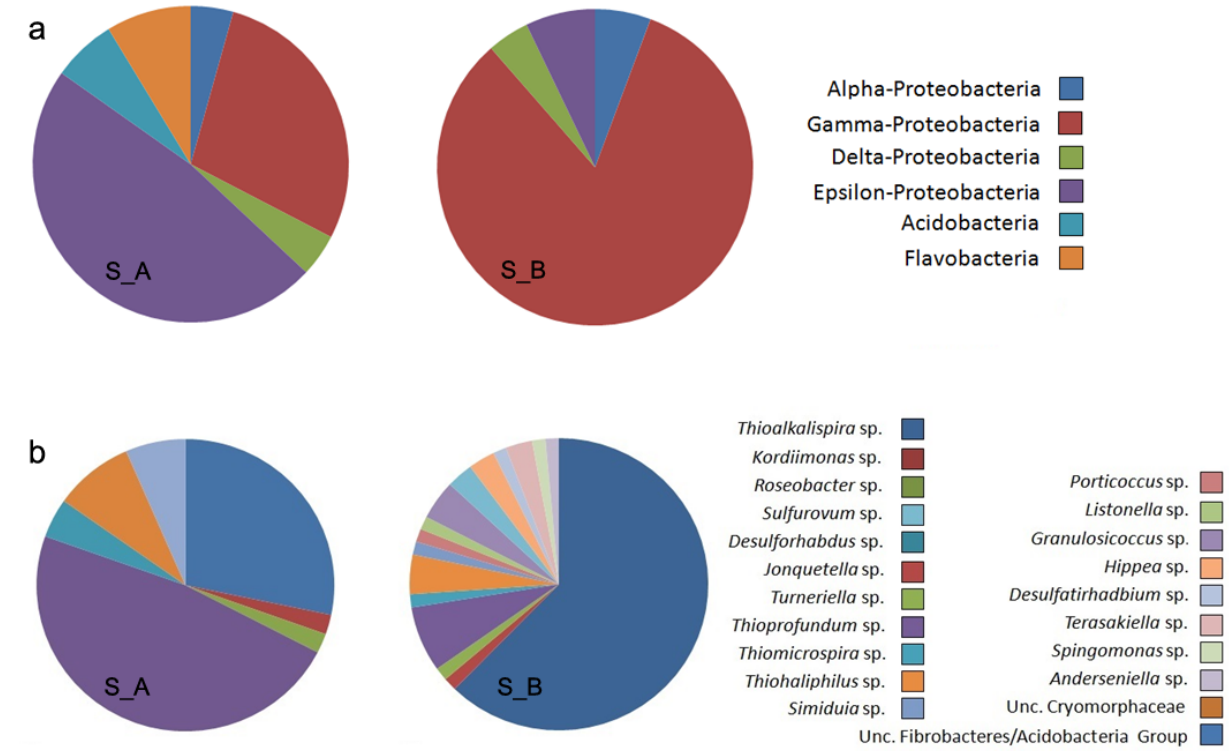

Figure 4

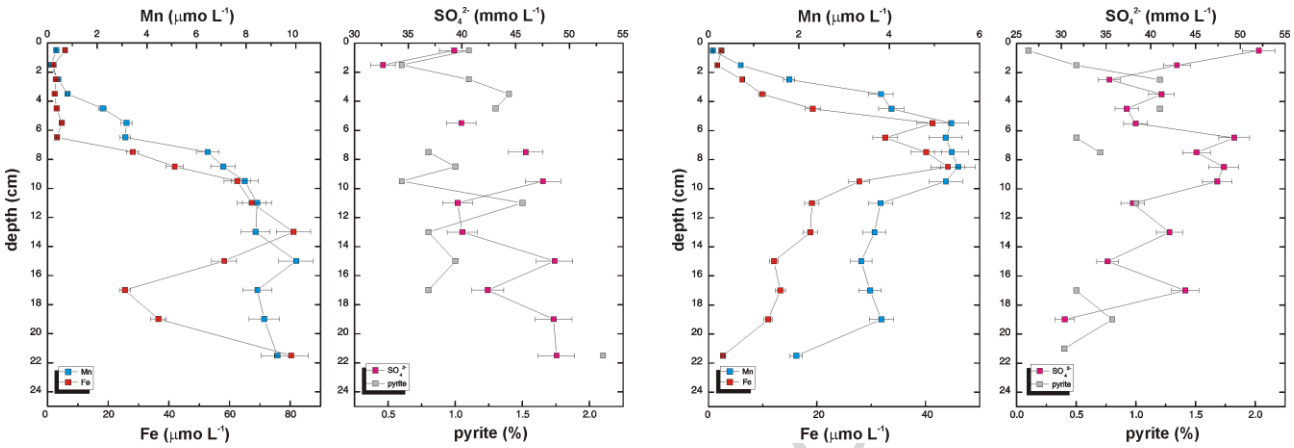

Figure 5

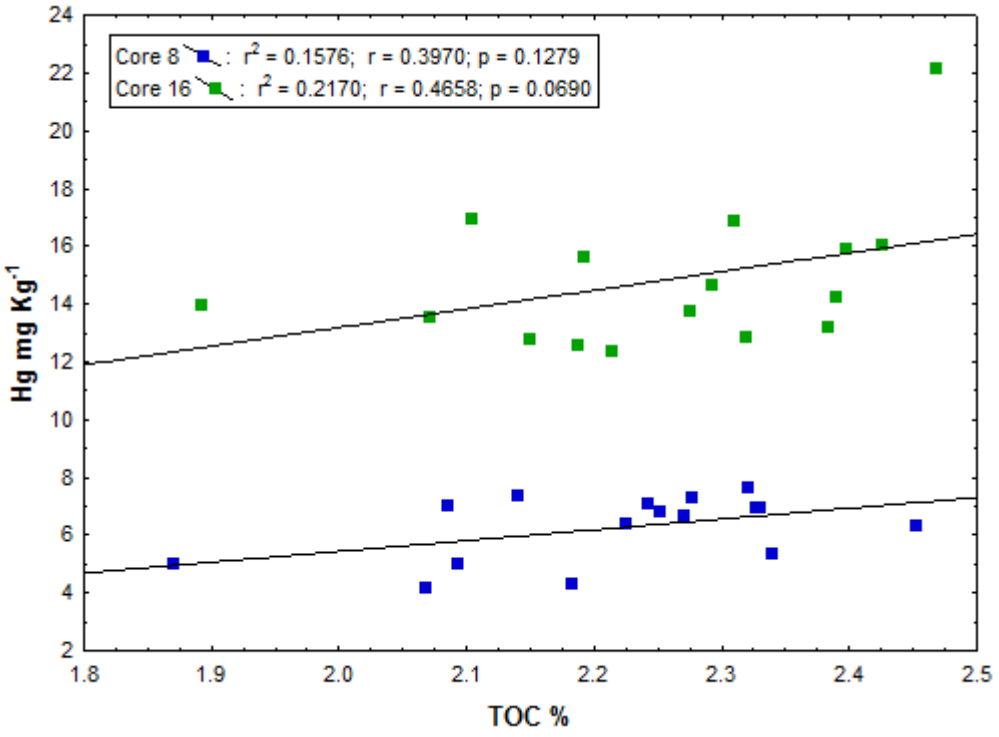

Figure 6

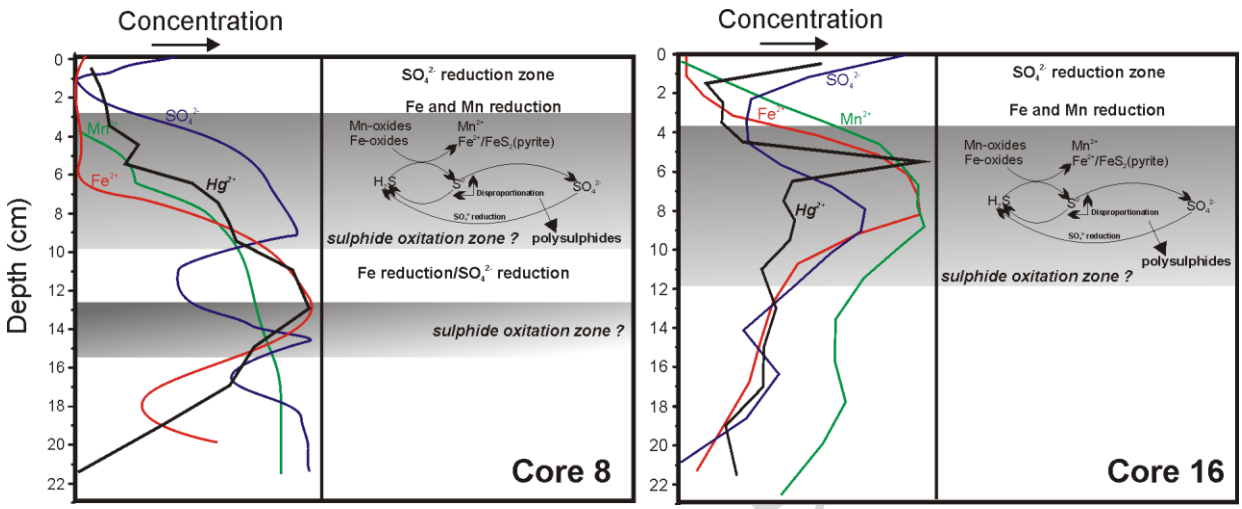

Figure 7

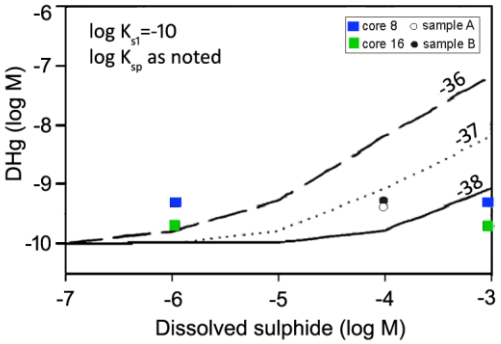

Figure 8

Table 1 Mean values and variation ranges of grain size fractions and mineralogy for the sediments from the Augusta box-cores.

		Core 8			Core 16		
		max	*min*	*mean*	*max*	*min*	*mean*
Grain size	clay	34	32	33	38	34	37
distribution (%)	silt	60	57	58	56	54	55
	sand	10	7	8	10	6	8
Mineralogy (%)	Clay minerals	46	20	33	50	10	34
	Quartz	21	14	34	22	9	16
	Calcite	52	25	17	55	29	37
	Plagioclase	14	< 1	5	6	2	4
	Hematite	9	4	5	8	3	5
	Dolomite	1	< 1	5	19	< 1	2
	Rhodochrosite	9	< 1	6	4	< 1	2
	Siderite	2	< 1	5			
	Pyrite	2	< 1	< 1	1	< 1	< 1

Table 2 Quantitative abundance of the microbial population for the sediments from the Augusta box-cores.

Sample	**THg mg kg^{-1}**	**Depth**	**DAPI (cell ml^{-1})**	**CFU$_{MA}$ (CFU ml^{-1})**	**MPN (cell ml^{-1})**
S_A (core 8)	7.36	13 cm	2.9 x 10^6	1.4 x 10^4	9.3 x10^2
S_B (core 16)	16.8	15 cm	5.8 x 10^6	3 x 10^4	4.3 x 10^3

Highlights

We describe factors controlling the pool of dissolved Hg in sediment pore waters

Fe-Mn reduction coupled to sulphide oxidation can favour the early diagenesis of Hg

An increase in HgS solubility is considered a key mechanism affecting Hg mobility

Thioalkalispira sulphur oxidizing bacteria can indirectly support HgS dissolution